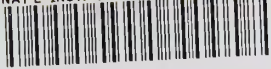


NATL INST. OF STAND & TECH R.I.C.



A11104 936148

NIST  
PUBLICATIONS

NISTIR 5816

## Electronics and Electrical Engineering Laboratory

J. M. Rohrbaugh  
Compiler

# Technical Publication Announcements

# 46

Covering Laboratory Programs,  
July to September 1995,  
with 1996 EEEL Events Calendar

U.S. DEPARTMENT OF COMMERCE  
Technology Administration  
National Institute of Standards  
and Technology

**NIST**

QC  
100  
.U56  
NO. 5816  
1996



NISTIR 5816

# Electronics and Electrical Engineering Laboratory

J. M. Rohrbaugh  
Compiler

Electronics and Electrical  
Engineering Laboratory  
Semiconductor Electronics Division  
Gaithersburg, MD 20899

# Technical Publication Announcements

April 1996

Covering Laboratory Programs,  
July to September 1995,  
with 1996 EEEL Events Calendar

# 46



U.S. DEPARTMENT OF COMMERCE  
Mary L. Good, Acting Secretary  
TECHNOLOGY ADMINISTRATION  
Gary R. Bachula, Acting Under  
Secretary for Technology  
NATIONAL INSTITUTE OF STANDARDS  
AND TECHNOLOGY  
Arati Prabhakar, Director



## INTRODUCTION TO THE EEEL TECHNICAL PUBLICATION ANNOUNCEMENTS

This is the forty-sixth issue of a quarterly publication providing information on the technical work of the National Institute of Standards and Technology Electronics and Electrical Engineering Laboratory (EEEL). This issue of the EEEL Technical Publication Announcements covers the third quarter of calendar year 1995.

Organization of Bulletin: This issue contains citations and abstracts for Laboratory publications published in the quarter. Entries are arranged by technical topic as identified in the Table of Contents and alphabetically by first author within each topic. Following each abstract is the name and telephone number of the individual to contact for more information on the topic (usually the first author). This issue also includes a calendar of Laboratory conferences and workshops planned for calendar year 1996 and a list of sponsors of the work.

Electronics and Electrical Engineering Laboratory: EEEL programs provide national reference standards, measurement methods, supporting theory and data, and traceability to national standards. The metrological products of these programs aid economic growth by promoting equity and efficiency in the marketplace, by removing metrological barriers to improved productivity and innovation, by increasing U.S. competitiveness in international markets through facilitation of compliance with international agreements, and by providing technical bases for the development of voluntary standards for domestic and international trade. These metrological products also aid in the development of rational regulatory policy and promote efficient functioning of technical programs of the Government.

The work of the Laboratory is conducted by five technical research Divisions: the Semiconductor Electronics and the Electricity Divisions in Gaithersburg, Md., and the Electromagnetic Fields, Electromagnetic Technology Divisions, and the newly formed Optoelectronics Division in Boulder, Colo. The Office of Law Enforcement Standards conducts research and provides technical services to the U.S. Department of Justice and State and local governments, and other agencies in support of law enforcement activities. In addition, the Office of Microelectronics Programs (OMP) coordinates the growing number of semiconductor-related research activities at NIST. Reports of work funded through the OMP are included under the heading "Semiconductor Microelectronics."

Key contacts in the Laboratory are given on the inside back cover; readers are encouraged to contact any of these individuals for further information. To request a subscription or for more information on the Bulletin, write to EEEL Technical Progress Bulletin, National Institute of Standards and Technology, Metrology Building, Room B-358, Gaithersburg, MD 20899 or call (301) 975-2220.

Laboratory Sponsors: The Laboratory Programs are sponsored by the National Institute of Standards and Technology and a number of other organizations, in both the Federal and private sectors; these are identified on page 20.

Note on Publication Lists: Publication lists covering the work of each division are guides to earlier as well as recent work. These lists are revised and reissued on an approximately annual basis and are available from the originating division. The current set is identified in the Additional Information section, page 18.

---

Certain commercial equipment, instruments, or materials are identified in this paper in order to specify adequately the experimental procedures. Such identification does not imply recommendation or endorsement by the National Institute of Standards and Technology, nor does it imply that the materials or equipment identified are necessarily the best available for the purpose.



## TABLE OF CONTENTS

INTRODUCTION .....	ii
To Learn More About the Laboratory .....	2
FUNDAMENTAL ELECTRICAL MEASUREMENTS .....	3
SEMICONDUCTOR MICROELECTRONICS .....	3
Silicon Materials [includes SIMOX and SOI] .....	3
Compound Materials .....	4
Analysis and Characterization Techniques .....	5
Device Physics and Modeling .....	5
Dimensional Metrology .....	6
Integrated-Circuit Test Structures .....	6
Microfabrication Technology [includes MBE, micromachining, MEMs] .....	6
Plasma Processing .....	6
SIGNAL ACQUISITION, PROCESSING, AND TRANSMISSION .....	8
Cryoelectronic Metrology .....	8
Antenna Metrology [includes radar cross section measurements] .....	10
Noise Metrology .....	10
Microwave and Millimeter-Wave Metrology .....	11
Electromagnetic Properties .....	11
Laser Metrology .....	11
Optical Fiber Metrology .....	12
Optical Fiber/Waveguide Sensors .....	12
Integrated Optics [includes waveguide structures] .....	13
Other Signal Topics .....	14
ELECTRICAL SYSTEMS .....	14
Power Systems Metrology .....	14
Superconductors .....	15
Other Electrical Systems Topics .....	17
ELECTROMAGNETIC INTERFERENCE .....	18
Conducted EMI .....	18
ADDITIONAL INFORMATION .....	18
Announcements .....	18
Lists of Publications .....	19
1996 Calendar of Events .....	20
EEEL Sponsors .....	20
NIST Silicon Resistivity SRMs .....	22

## TO LEARN MORE ABOUT THE LABORATORY....

Two general documents are available that may be of interest. These are *Measurements for Competitiveness in Electronics* and *EEEL 1994 Technical Accomplishments, Supporting Technology for U.S. Competitiveness in Electronics*. The first identifies measurement needs for a number of technical areas and the general importance of measurements to competitiveness issues. The findings of each chapter dealing with an individual industry have been reviewed by members of that industry. The second presents selected technical accomplishments of the Laboratory for the period October 1, 1993 through September 30, 1994. A brief indication of the nature of the technical achievement and the rationale for its undertaking are given for each example. A longer description of both documents follows:

### **Measurements for Competitiveness in Electronics, NISTIR 4583 (April 1993).**

*Measurements for Competitiveness in Electronics* identifies for selected technical areas the measurement needs that are most critical to U.S. competitiveness, that would have the highest economic impact if met, and that are the most difficult for the broad range of individual companies to address. The document has two primary purposes: (1) to show the close relationship between U.S. measurement infrastructure and U.S. competitiveness and show why improved measurement capability offers such high economic leverage, and (2) to provide a statement of the principal measurement needs affecting U.S. competitiveness for given technical areas, as the basis for a possible plan to meet those needs, should a decision be made to pursue this course.

The first three chapters, introductory in nature, cover the areas of: the role of measurements in competitiveness, NIST's role in measurements, and an overview of U.S. electronics and electrical-equipment industries. The remaining nine chapters address individual fields of electronic technology: semiconductors, magnetics, superconductors, microwaves, lasers, optical-fiber communications, optical-fiber sensors, video, and electromagnetic compatibility. Each of these nine chapters contains four basic types of information: technology review, world markets and U.S. competitiveness, goals of U.S. industry for competitiveness, and measurement needs. Three appendices provide definitions of the U.S. electronics and electrical-equipment industries.

This document is a successor to NISTIR 90-4260, *Emerging Technologies in Electronics ... and their measurement needs* [Second Edition].

[Contact: Ronald M. Powell, (301) 975-2220]

### **EEEL 1994 Technical Accomplishments, Supporting Technology for U.S. Competitiveness in Electronics, NISTIR 5551 (December 1994).**

The Electronics and Electrical Engineering Laboratory, working in concert with other NIST Laboratories, is providing measurement and other generic technology critical to the competitiveness of the U.S. electronics industry and the U.S. electricity-equipment industry. This report summarizes selected technical accomplishments and describes activities conducted by the Laboratory in FY 1994 in the field of semiconductors, magnetics, superconductors, low-frequency microwaves, lasers, optical fiber communications and sensors, video, power, electromagnetic compatibility, electronic data exchange, and national electrical standards. Also included is a profile of EEEL's organization, its customers, and the Laboratory's long-term goals.

EEEL is comprised of five technical divisions, Electricity and Semiconductor Electronics in Gaithersburg, Maryland, and Electromagnetic Fields, Electromagnetic Technology, and Optoelectronics in Boulder, Colorado. Through two offices, the Laboratory manages NIST-wide programs in microelectronics and law enforcement.

[Contact: JoAnne Surette, (301) 975-5267]

**Internet Access (World Wide Web): <http://www.eeel.nist.gov>**



## FUNDAMENTAL ELECTRICAL MEASUREMENTS

Lee, K.C., **The Quantum Hall Effect-Based Resistance Standard: Capabilities and Implementation**, Proceedings of the Eighteenth Annual Workshop of NASA Metrology and Calibration 1995, Greenbelt, Maryland, April 18-20, 1995, Section 6, pp. 1-6.

In order to support modern 8 1/2-digit digital multimeters and high-accuracy calibrators capable of delivering uncertainties of the order of parts per million (ppm), primary standards laboratories must be able to provide calibration uncertainties less than 0.1 ppm. Quantum Hall effect-based resistance standards can provide these low uncertainties, but at present require very sophisticated and costly equipment. This talk describes the quantum Hall effect (QHE), the equipment necessary to use it as a resistance standard, and some of the challenges in making a QHE-based resistance standard commercially viable.

[Contact: Kevin C. Lee, (301) 975-4236]

## SEMICONDUCTOR MICROELECTRONICS

### Silicon Materials

Jacobs, C., Genis, A., Allen, L.P., and Roitman, P., **Effect of Anneal Temperature on Si/Buried Oxide Interface Roughness of SIMOX**, Proceedings of the 1994 IEEE SOI Conference, Nantucket, Massachusetts, October 3-6, 1994, pp. 49-50 (1995).

Fully depleted, thin-film silicon-on-insulator (SOI) SIMOX devices are attractive for their short-channel characteristics and high speed compared with bulk silicon. Their potential for applications in low power devices and circuitry places extreme demands upon the starting SIMOX substrate material. Threshold voltage control for fully depleted SOI devices has been recognized as a key issue for realization of fully depleted SOI technology. To that end, examination of the interface roughness between the device silicon layer and the buried oxide of the SOI structure is an active area of materials research and development. In this work, we have used atomic force microscopy to measure the interface roughness of SIMOX SOI substrates as a function of anneal parameters. This study has shown that the

silicon/buried oxide interface roughness is a strong function of the post-implant annealing temperature. [Contact: Peter Roitman, (301) 975-2077]

Kopanski, J.J., **Oxidation of SiC**, in Properties of Silicon Carbide, Chapter 5.2, G. L. Harris, Ed. (INSPEC, the Institution of Electrical Engineers, London, United Kingdom, 1995), pp. 121-129.

Thermal oxidation of the two most common forms of single-crystal silicon carbide with potential for semiconductor electronics applications is discussed: 3C-SiC formed by heteroepitaxial growth by chemical vapor deposition on silicon, and 6H-SiC wafers grown in bulk by vacuum sublimation or the Lely method. SiC is also an important ceramic and abrasive that exists in many different forms. Its oxidation has been studied under a wide variety of conditions. Thermal oxidation of SiC for semiconductor electronic applications is discussed. Insulating layers on SiC, other than thermal oxide, and the electrical properties of the thermal oxide and metal-oxide-semiconductor capacitors formed on SiC are also discussed.

[Contact: Joseph J. Kopanski, (301) 975-2089]

Lee, J.D., Park, J.C., Krause, S., and Roitman, P., **Defect Formation Mechanism Causing Increasing Defect Density During Decreasing Implant Dose in Low-Dose SIMOX**, Proceedings of the 1994 IEEE SOI Conference, Nantucket, Massachusetts, October 3-6, 1994, pp. 69-70 (1995).

Silicon-on-insulator material synthesized by oxygen implantation (SIMOX) is a leading candidate for advanced large-scale integrated-circuit applications due to thickness uniformity and moderate defect density. In the past few years, there has been a significant reduction of the defect density by optimizing processing conditions. Today, commercial SIMOX wafers are available by single implant at a high dose of  $1.8 \times 10^{18} \text{ cm}^{-2}$  (defect density  $\sim 10^6 \text{ cm}^{-2}$ ), single implant at a low dose of  $\sim 0.5 \times 10^{18} \text{ cm}^{-2}$  (defect density  $< 10^3 \text{ cm}^{-2}$ ), and multiple implants/anneals (defect density  $< 10^4 \text{ cm}^{-2}$ ). Studies on defect formation mechanisms may suggest further modification of the processing conditions for both production cost and material quality. Recently, it was shown that through-thickness defects in high-dose SIMOX originated from as-implanted defects, dislocation half-loops.

On the other hand, a high density ( $\sim 10^8 \text{ cm}^{-2}$ ) of defects has not been understood. In this paper, we report on the effect of implant dose on defect formation mechanisms, and propose a defect formation mechanism in very low-dose regime for the first time.

[Contact: Peter Roitman, (301) 975-2077]

Sadana, D.K., Lasky, J., Hovel, H.J., Petrillo, K., and Roitman, P., **Nano-Defects in Commercial Bonded SOI and SIMOX**, Proceedings of the 1994 IEEE SOI Conference, Nantucket, Massachusetts, October 3-6, 1994, pp. 111-112.

Two new classes of defects have been identified in commercial Separation by IMplantation of OXYgen (SIMOX), plasma thinned bonded silicon-on-insulator (BSOI) and bonded etched silicon-on-insulator (BESOI) materials. The first class of defects is revealed when the materials are treated in concentrated HF, and their density is in the range  $10^2$  to  $10^3 \text{ cm}^{-2}$ . The second class of defects appears when the materials are etched by the enhanced Secco etch method. Contrary to the common belief, defect densities of  $10^4$  to  $10^5 \text{ cm}^{-2}$  are present in both plasma-thinned BSOI and BESOI after Secco etching. The defect densities in SIMOX after the Secco etching were  $10^6$  to  $10^7 \text{ cm}^{-2}$ , which was expected.

[Contact: Peter Roitman, (301) 975-2077]

Twigg, M.E., Hughes, H.L., Roitman, P., and Allen, L.P., **Measurement of Low Defect Densities in SIMOX Using Transmission Electron Microscopy**, Proceedings of the 1994 IEEE SOI Conference, Nantucket, Massachusetts, October 3-6, 1994, pp. 85-86 (1995).

In order to reduce short-channel effects for devices with channel lengths less than  $0.25 \mu\text{m}$ , the buried oxide (BOX) thickness will need to be less than 200 nm. To this end, an experimental low-dose ( $0.7 \times 10^{18}/\text{cm}^2$ ) oxygen implantation process for thin-BOX SIMOX has been explored. The extended defects in this material are predominantly dislocation pairs that run from the superficial Si/BOX interface to oxide precipitates. As in all electronic materials, the dislocation density in the device region must also be minimized. A reduction in the superficial Si layer dislocation density from  $\sim 10^7/\text{cm}^2$  to an estimated

value of less than  $100/\text{cm}^2$  was achieved by subjecting this material to prolonged (16-h) anneal at  $1325 \text{ }^\circ\text{C}$  in an atmosphere of 0.5%  $\text{O}_2$  in Ar. The anneal effectively reduced the device silicon layer from 270 nm to 200 nm as measured by cross-sectional TEM. The BOX layer thickness was unchanged by the anneal and remained at 130 nm.

[Contact: Peter Roitman, (301) 975-2077]

### Compound Materials

Bennett, H.S., **Summary Report of the Workshop on Planning for Compound Semiconductor Technology**, NISTIR 5702 (August 1995).

This report describes the motivation for and the results of the Workshop on Planning for Compound Semiconductor Technology. It also includes copies of the viewgraphs used by the speakers at the Workshop. This Workshop, sponsored by the National Institute of Standards and Technology and the Semiconductor Equipment and Materials International, was held at Gaithersburg, Maryland on February 3, 1995.

The purposes of the Workshop were to assess whether agreement exists in the compound semiconductor industry on the need for a consensus-based planning effort and to foster the free exchange of information and ideas that might be used to create a more competitive compound semiconductor industry.

The Workshop attendees agreed that a consensus on the need for such planning does exist, and that if such planning occurs, it is more appropriate to use existing industry and government organizations. The attendees also proposed the four future actions of 1) forming an industrial alliance on planning for compound semiconductors; 2) coordinating the activities of the proposed compound semiconductor alliance with related activities in government agencies; 3) determining to what extent the government agencies and other interested parties are able to provide funds and/or staff to form the compound semiconductor alliance; and 4) forming a parallel organization for the microwave/radio frequency industry that addresses questions similar to those addressed by Optoelectronics Industry Development Association for optoelectronics.

[Contact: Herbert S. Bennett, (301) 975-2079]

Kim, J.S., Seiler, D.G., Colombo, L., and Chen, M.C., **Characterization of Liquid-Phase Epitaxially Grown HgCdTe Films by Magnetoresistance Measurements**, *Journal of Electronic Materials*, Vol. 24, No. 9, pp. 1305-1310 (1995).

In this paper, we demonstrate that measurements of the magnetoresistance can be used as a valuable alternative to conventional characterization tools to study transport properties of advanced semiconducting materials, structures, or devices. We have measured magnetoresistance on two different systems, namely, three liquid-phase epitaxially grown HgCdTe films and two GaAs-based high-electron-mobility-transistor (HEMT) structures. The results are analyzed by using a two-carrier model as a reference in the context of the reduced-conductivity-tensor scheme. The HEMT data are in quantitative agreement with the two-carrier model, but the HgCdTe data exhibit appreciable deviations from the model. The observed deviations strongly indicate a mobility spread and material complexity in the HgCdTe samples which are probably associated with inhomogeneities and the resulting anomalous electrical behavior.

[Contact: Jin S. Kim, (303) 975-2238]

#### Analysis and Characterization Techniques

Dagata, J.A., and Kopanski, J.J., **Scanning Probe Techniques for the Electrical Characterization of Semiconductor Devices**, *Solid State Technology*, pp. 91-97 (July 1995).

The spatial resolution, sensitivity, and accuracy required for electrical characterization of device structures in the semiconductor industry suggest that scanning probe microscopy (SPM) tools may offer an alternative to existing measurement techniques. Due to their two-dimensional imaging capabilities, high-spatial resolution, and nondestructive nature, SPM-based characterization tools are evolving from lab to fab. This article examines the current standard of performance for electrical measurements of semiconductor devices and the prospects for the application of SPM as a next-generation tool for dopant profiling and defect inspection of device structures.

[Contact: Joseph J. Kopanski, (301) 975-2089]

Schaafsma, D.T., and Christensen, D.H., **Cross-**

**Sectional Photoluminescence and Its Application to Buried-Layer Semiconductor Structures**, *Journal of Applied Physics*, Vol. 78, No. 2, pp. 694-699 (July 15, 1995).

We present an overview of a cross-sectional scanning microphotoluminescence technique. This technique is used to examine various buried-layer semiconductor structures for which traditional surface-normal techniques cannot yield sufficient information or must be coupled with time-consuming and painstaking processes such as wet etching. This technique has a wide range of applications; two applications, defect-driven interdiffusion in quantum wells and the modification of spontaneous emission from quantum wells in vertical-cavity surface-emitting lasers (VCSELs), are discussed here. The data obtained using this method can be used to distinguish emission spectra from quantum wells as little as 1  $\mu\text{m}$  apart in depth and a few nanometers different in wavelength. The comparison of normal-incidence with cross-sectional data from VCSELs can be used to more effectively optimize the match between cavity resonance and quantum-well emission in high-Q devices. The physical model for an oscillating dipole in a planar cavity leads to an interesting conclusion about the dependence of the emission spectrum on the location of the dipole, namely, that an emitter inside a Fabry-Perot cavity will have the same spectrum as an identical one located a corresponding distance outside of the cavity. This conclusion is tested experimentally, using a VCSEL structure with emitters distributed inside and outside the effective cavity length.

[Contact: David H. Christensen, (303) 497-3354]

#### Device Physics and Modeling

Lowney, J.R., **Model for Determining the Density and Mobility of Carriers in Thin Semiconducting Layers with Only Two Contacts**, *Journal of Applied Physics*, Vol. 78, No. 2, pp. 1008-1012 (15 July 1995).

A new method for determining the carrier densities and mobilities in a thin semiconducting layer was recently described. It is based on fitting the transverse magnetoresistance of the layers as a function of magnetic field, and it requires only two contacts. To improve the accuracy and generalize

the procedure to multicarrier systems, a computer code was written to solve for the magnetoresistance as a function of magnetic field and the length-to-width ratio of a rectangular sample. A nonlinear least-squares fit was made to the results of the computer model for a single-carrier system. The results for multi-carrier systems are discussed. This method is especially useful as a monitor for improving the quality control of the electrical characteristics of thin conducting layers in finished devices. The code is also useful for interpreting standard four-terminal measurements as well.

[Contact: Jeremiah R. Lowney, (301) 975-2048]

### Dimensional Metrology

Lowney, J.R., **MONSEL-II Monte Carlo Simulation of SEM Signals for Linewidth Metrology**, *Microbeam Analysis*, Vol. 4, pp. 131-136 (1995).

This is a guide to the FORTRAN code MONSEL-II, which is a Monte Carlo simulation of the transmitted, backscattered, and secondary electron signals in a scanning electron microscope (SEM) associated with lines with a trapezoidal cross section. The lines are deposited on a multilayer substrate. The primary purpose of the code is to interpret the actual linewidths from measured SEM signals. However, it can be used for many other purposes such as transmission electron microscopy.

[Contact: Jeremiah R. Lowney, (301) 975-2048]

### Integrated-Circuit Test Structures

Schuster, C.E., **Semiconductor Measurement Technology: Test Structure Implementation Document: DC Parametric Test Structures and Test Methods for Monolithic Microwave Integrated Circuits (MMICs)**, NIST Special Publication 400-97 (September 1995).

This document describes a set of microelectronic test structure designs for manufacturers of GaAs MMIC devices. These designs enable the dc measurement of process and device parameters that can be used to diagnose, monitor, compare, and predict the performance of the fabrication process or the devices produced. The test structure designs are embodied in a computer-aided design library known at NISTGAAS, which contains eight types of test structures, implemented in 125

combinations of process layer and size, and based on a 2 x 6 probe-pad array. Any design, once fabricated on a wafer, can be probed using commonly available commercial parametric test system equipment. This document specifies how to implement and test each type of test structure and how to analyze the results. It also provides guidance on how to apply the set of test structures at the wafer level. Although NISTGAAS was designed for the process described in this document, it was also designed and demonstrated to be adaptable for other MMIC processes. Since NISTGAAS contains cell designs rather than a chip design, it provides a flexible test structure methodology that also provides the MMIC community with a common reference point for assessing process and device performance.

[Contact: Constance E. Schuster, (301) 975-2241]

### Microfabrication Technology

Gaitan, M., **MEMS in Standard CMOS VLSI Technology**, *Proceedings of the Twenty-Ninth Annual Conference on Information Sciences and Systems*, Baltimore, Maryland, March 22-24, 1995, pp. 169-173.

The methodology for the design and fabrication of a class of thermo-electro-mechanical devices and systems that can be fabricated in a commercial CMOS foundry environment is presented. The fabrication technique allows the monolithic integration of the micromechanical devices with CMOS VLSI circuits using standard design methods. Microheating elements and thermoelectric sensors are presented as examples of the application of this technique.

[Contact: Michael Gaitan, (301) 975-2070]

### Plasma Processing

Olthoff, J.K., Van Brunt, R.J., and Radovanov, S.B., **Effect of Electrode Material on Measured Ion Energy Distributions in Radio-Frequency Discharges**, *Applied Physics Letters*, Vol. 67, No. 4, pp. 473-475 (July 24, 1995).

The influence of electrode surface material and conditions on the measurement of kinetic-energy distributions of ions sampled through an orifice in the grounded electrode of a parallel-plate, capaci-

tively-coupled radio-frequency discharge cell has been investigated for discharges generated in different gas mixtures. Significant shifts in energy and/or discrimination of low-energy ions are observed for aluminum electrodes or for stainless-steel electrodes on which aluminum appears to have been deposited by sputtering. Their effects are considerably reduced in the case of stainless-steel electrodes that have been freshly cleaned and polished. It is argued that the observed energy shifts are attributable to charging of oxide layers on the electrode surface around the sampling orifice.

[Contact: James K. Olthoff, (301) 975-2431]

Radovanov, S.B., Olthoff, J.K., Van Brunt, R.J., and Djurovic, S., **Ion Kinetic-Energy Distributions and Balmer-alpha ( $H_\alpha$ ) Excitation in Ar- $H_2$  Radio-Frequency Discharges**, *Journal of Applied Physics*, Vol. 78, No. 2, pp. 746-757 (July 15, 1995).

Excited neutrals and fast ions produced in a 13.56 MHz radio-frequency discharge in a 90% argon - 10% hydrogen gas mixture were investigated, respectively, by spatially and temporally resolved optical emission spectroscopy, and by mass-resolved measurements of ion kinetic energy distributions at the grounded electrode. The electrical characteristics of the discharge were also measured, and comparisons are made with results obtained for discharges in pure  $H_2$  under comparable conditions. Measurements of Balmer-alpha ( $H_\alpha$ ) emission show Doppler-broadened emission that is due to the excitation of fast atomic hydrogen neutrals formed with ion neutralization processes in the discharge. Temporally and spatially resolved emission profiles of the  $H_\alpha$  radiation from the Ar- $H_2$  mixture are presented for the "slow" component produced predominately by electron-impact dissociative excitation of  $H_2$ , and for the "fast" component corresponding to energies much greater than can be derived from dissociative excitation. For the Ar- $H_2$  mixture, the fast component is significantly enhanced relative to the slow component. The measured, kinetic-energy distributions and fluxes of predominant ions in the Ar- $H_2$  mixture, such as  $H_3^+$ ,  $H_2^+$ ,  $H^+$ , and  $ArH^+$ , suggest mechanisms for the formation of fast hydrogen atoms. The interpretation of results indicate that  $H^+$  and/or  $H_3^+$ , neutralized and backscattered by collision with the powered electrode, are the likely sources of fast

hydrogen atoms that produce Doppler-shifted  $H_\alpha$  emission in the discharge. There is also evidence at the highest pressures and voltages of "runaway"  $H^+$  ions formed near the powered electrode, and detected with kinetics energies exceeding 100 eV at the grounded electrode.

[Contact: Svetlana B. Radovanov, (301) 975-2436]

Rao, M.V.V.S., Radovanov, S.B., Van Brunt, R.J., and Olthoff, J.K., **Kinetic Energy Distribution of Ions Produced from Townsend Discharges in Neon and Argon**, *Proceedings of the Nineteenth International Conference on Physics of Electronic and Atomic Collisions*, Whistler, British Columbia, Canada, July 26—August 1, 1995, p. 392.

Study of the kinetic energy distribution (KED) of various ions produced in the breakdown of a gas under the influence of a uniform dc electric field at various electric field to gas density (E/N) ratios provides important information on the relative role of elastic and inelastic collision processes which occur in transporting ions within the discharge sheath region. In this paper, we present our results on the measurements of KEDs of  $Ne^+$  in Ne and  $Ar^+$  in a low-current diffuse Townsend discharges. The discharges are generated between two plane and circular parallel plates. The discharge cell is coupled to a cylindrical mirror analyzer (CMA) in conjunction with a quadrupole mass spectrometer (QMS). The ions sampled through a 0.1 mm orifice at the center of the discharge are energy analyzed by the CMA, and subsequently, separated according to their mass to charge ratio (m/z) by the QMS. More details on the apparatus and data acquisition system have been discussed elsewhere.

[Contact: Richard J. Van Brunt, (301) 975-2425]

Van Brunt, R.J., Olthoff, J.K., and Radovanov, S.B., **Influence of Electrode Material on Measured Ion Kinetic-Energy Distributions in Radio-Frequency Discharges**, *Proceedings of the XXII International Conference on Phenomena in Ionized Gases*, Hoboken, New Jersey, July 31—August 4, 1995, pp. 29-30.

The measurement of ion kinetic energies is important for understanding processes that occur in discharges, e.g., the influence of ions on the etching of semiconductor materials in plasma reactors. Direct measurements of ion kinetic energies striking

surfaces exposed to the discharge requires sampling through an orifice in a surface. Difficulties with ion sampling through a small aperture, manifested by errors or distortions in measured ion kinetic-energy distributions, have been encountered in previous investigations of both dc and radio-frequency discharges. The errors are usually most significant at relatively low ion energies.

[Contact: Richard J. Van Brunt, (301) 975-2425]

## SIGNAL ACQUISITION, PROCESSING, AND TRANSMISSION

### Cryoelectronic Metrology

Benz, S.P., Reintsema, C.D., and Ono, R.H., **Step-Edge and Stacked-Heterostructure High- $T_c$  Josephson Junctions**, IEEE Transactions on Applied Superconductivity, Vol. 5, No. 2, pp. 2915-2918 (June 1995).

We have explored two high-transition-temperature Josephson junction technologies for application in voltage standard arrays: step-edge junctions made with  $\text{YBa}_2\text{Cu}_3\text{O}_{7-\delta}$  and Au normal-metal bridges, and stacked series arrays of Josephson junctions in selectively doped, epitaxially grown  $\text{Bi}_2\text{Sr}_2\text{CaCu}_2\text{O}_8$  heterostructures. For both kinds of junctions, Shapiro steps induced by a microwave bias were characterized as a function of power. We compare the two technologies with respect to critical current and normal resistance uniformity, maximum achievable critical current, critical-current normal-resistance product, and operating temperature.

[Contact: Samuel P. Benz, (303) 497-5258]

Booi, P.A.A., and Benz, S.P., **Resonances in Two-Dimensional Array Oscillator Circuits**, IEEE Transactions on Applied Superconductivity, Vol. 5, No. 2, pp. 2899-2902 (June 1995).

We present experimental results on the emission from phase-locked two-dimensional arrays of Josephson junctions. We have coupled the emission from  $10 \times 10$  arrays to a room-temperature mixer through a fin-line antenna and WR-12 waveguide. A single voltage-tunable peak was detected up to 230 GHz. A stripline resonance in the antenna reduced the array's dynamic resistance and, thereby, the emission linewidth to as low as 10 kHz. We extract an effective noise temperature of

14 K from the linewidth data. When the array's emission was coupled to an on-chip detector junction through a dc blocking capacitor, we detected voltage-tunable emission from 75 GHz to 300 GHz, and in some circuits, emission above 400 GHz. Here, the coherent power spectrum depends primarily on internal resonances.

[Contact: Peter A. A. Booi, (303) 497-5910]

Doderer, T., Lachenmann, S.G., Huebener, R.P., Booi, P.A.A., and Benz, S.P., **Direct Observation of Vortex Dynamics in Two-Dimensional Josephson-Junction Arrays**, IEEE Transactions on Applied Superconductivity, Vol. 5, No. 2, pp. 2723-2726 (June 1995).

Spatially resolved images of the dynamic states of current-biased overdamped two-dimensional arrays of  $\text{Nb}/\text{AlO}_x/\text{Nb}$  Josephson junctions were obtained using low-temperature scanning electron microscopy. We present two-dimensional imaging results describing various vortex dynamic regimes in zero applied magnetic field. The nucleation of current-induced vortices at the array boundaries and their subsequent motion into the array interior are observed for bias currents slightly above the array critical current. With increasing bias current, vortex-vortex interaction becomes important. Discussions on the coherent microwave radiation emission are presented.

[Contact: Peter A. A. Booi, (303) 497-5910]

Eckstein, J.N., Bozovic, I., Virshup, G.F., Ono, R.H., and Benz, S.P., **Stacked Series of High- $T_c$  Trilayer Josephson Junctions**, IEEE Transactions on Applied Superconductivity, Vol. 5, No. 2, pp. 3284-3287 (June 1995).

We report on the properties of stacked series arrays of trilayer Josephson junctions grown by atomic layer-by-layer molecular beam epitaxy. Trilayer Josephson junctions oriented so that the current travels in the c-axis direction have been described previously. Series arrays are made by placing more than one barrier layer in the BSCCO-based epitaxial structure. Single molecular layers of BSCCO-2212 doped with Dy to reduce the local carrier concentration are used as barriers, and are placed very close to each other, e.g., separated by only a few molecular layers of the superconducting phase. Phase locking of ac Josephson currents has been

observed. The critical current density of such junctions has been observed to be very uniform on wafers that are free of second-phase defects, and operation up to 60 K has been obtained.

[Contact: Ronald H. Ono, (303) 497-3762]

Grossman, E.N., Vale, L.R., Rudman, D.A., Zink, L.R., and Evenson, K.M., **30 THz Mixing Experiments on High Temperature Superconducting Josephson Junctions**, IEEE Transactions on Applied Superconductivity, Vol. 5, No. 2, pp. 3061-3064 (June 1995).

We have investigated  $\text{YBa}_2\text{Cu}_3\text{O}_{7-\delta}$  superconductor-normal-superconductor Josephson junctions as mixers of 30 THz radiation. We have directly observed (second-order) difference frequencies from 10 MHz to 12.8 GHz between two  $\text{CO}_2$  laser lines. Applying a third microwave signal to the junction, we have observed  $\text{CO}_2$  laser difference frequencies up to 27 GHz. The dc bias dependence of the difference frequency signal, as well as other evidence, suggests two distinct mixing mechanisms: hot-electron mixing in the junction banks at high-dc biases, and bolometric Josephson mixing at low-dc biases. The latter is the first observation of Josephson mixing at  $\text{CO}_2$  laser frequencies in high- $T_c$  junctions. The Josephson mixing has generated observable mixing products up to sixth order.

[Contact: Erich N. Grossman, (303) 497-5102]

Irwin, K.D., Nam, S.W., Cabrera, B., Chugg, B., Park, S.G., Welty, R.P., and Martinis, J.M., **A Self-Biasing Cryogenic Particle Detector Utilizing Electrothermal Feedback and a SQUID Readout**, IEEE Transactions on Applied Superconductivity, Vol. 5, No. 2, pp. 2690-2693 (June 1995).

We are developing and testing a new type of superconducting transition edge sensor for phonon-mediated particle detection. This sensor consists of a superconducting tungsten thin film deposited on a silicon substrate. The temperature of the film is held constant within the superconducting transitions ( $T_c = 70$  mK) by a feedback process, with the substrate temperature well below the film temperature. Phonon energy deposited in the film is removed by a reduction in feedback Joule heating, which is measured using a series array of dc superconducting quantum interference devices.

The resulting signals show improvements in linearity and signal-to-noise ratio over our previous transition edge sensors.

[Contact: John M. Martinis, (303) 497-3597]

Kautz, R.L., **Phase Locking in Two-Dimensional Josephson Junction Arrays: Effect of Critical-Current Nonuniformity**, IEEE Transactions on Applied Superconductivity, Vol. 5, No. 2, pp. 2702-2706 (June 1995).

Numerical simulations are used to study mutual phase locking in two-dimensional arrays of Josephson junctions for parameters typical of successful millimeter-wave oscillators. Such arrays are shown to be very tolerant of random critical-current nonuniformities. However, comparison with an equivalent series array reveals that the locking between rows in a two-dimensional array is principally due to feedback through the external load and not to internal coupling between rows.

[Contact: Richard L. Kautz, (303) 497-3391]

Missert, N.N., Vale, L.R., Ono, R.H., Reintsema, C.D., Rudman, D.A., Thomson, R.E., and Berkowitz, S.J., **Temperature Dependence and Magnetic Field Modulation of Critical Currents in Step-Edge SNS YBCO/Au Junctions**, IEEE Transactions on Applied Superconductivity, Vol. 5, No. 2, pp. 2969-2972 (June 1995).

We compare the electrical transport properties of superconductor-normal metal-superconductor (SNS) step-edge YBCO/Au junctions where the Au is deposited at 100 °C and 600 °C. For both types of junctions, we observe resistively shunted junctions current-voltage characteristics. The critical currents  $I_c$  in all cases are similar for a given YBCO thickness to step height ratio, while the normal resistance  $R_n$  for the Au deposited at 600 °C is consistently 25% lower. The normalized temperature dependence of the  $I_c R_n$  product is identical for all junctions with Au deposited at high temperatures and varies among junctions on a single chop for Au deposited at 100 °C. Low magnetic field modulation of the critical current can show either the expected Fraunhofer-like pattern or a double-junction modulation for both types of devices. The modulation period is consistently a factor of three lower for the high-temperature deposited Au.

[Contact: Leila L. Vale, (303) 497-5121]

Reintsema, C.D., Ono, R.H., Barnes, G., Borchardt, L., Harvey, T.E., Kunkel, G., Rudman, D.A., Vale, L.R., Missert, N., and Rosenthal, P.A., **The Critical Current and Normal Resistance of High- $T_c$  Step-Edge SNS Junctions**, IEEE Transactions on Applied Superconductivity, Vol. 5, No. 2, pp. 3405-3409 (June 1995).

We have fabricated high- $T_c$  superconductor-normal-superconductor Josephson junctions with a variety of controlled geometries and measured the resulting dependences of critical current and normal resistance. These studies show that we can adjust our junction parameters over orders of magnitude, thus allowing us to tailor the junctions for a variety of applications.

[Contact: Carl D. Reintsema, (303) 497-5052]

Sauvageau, J.E., Booi, P.A.A., Cromar, M.W., Benz, S.P., Burroughs, C.J., and Koch, J.A., **Superconducting Integrated Circuit Fabrication Process Utilizing Low-Temperature ECR-Based PECVD  $\text{SiO}_2$  Dielectric Films**, IEEE Transactions on Applied Superconductivity, Vol. 5, No. 2, pp. 2303-2309 (June 1995).

A superconducting integrated circuit fabrication process has been developed to encompass a wide range of applications such as Josephson voltage standards, VLSI scale array oscillators, SQUIDs, and kinetic-inductance-based devices. An optimal Josephson junction process requires low-temperature processing for all deposition and etching steps. This low-temperature process involves an electron-cyclotron-resonance-based plasma-enhanced chemical vapor deposition (PECVD) of  $\text{SiO}_2$  films for interlayer dielectrics. Experimental design and statistical process control techniques have been used to ensure high-quality oxide films. Oxide and niobium etch processes include endpoint detection and controlled overetch of all films. An overview of the fabrication process is presented.

[Contact: Joseph E. Sauvageau, (303) 497-3770]

### Antenna Metrology

Lewis, R.L., **Spherical-Wave Source-Scattering Matrix Analysis of Antennas and Antenna-Antenna Interactions**, NIST Technical Note 1373 (July 1995).

Expressions are presented for describing incoming and outgoing fields about an antenna in terms of a series of exciting and emergent vector spherical-wave functions. The exciting and emergent fields around the antenna's exterior are related to the field in the antenna feed through a source-scattering matrix representation. Series of spherical-wave source-scattering matrix coefficients are used to express more conventional antenna parameters such as gain and receiving cross section. An overview of rotation and translation theorems for transforming vector spherical-wave functions between two distinct coordinate systems is given, followed by a general solution to the problem of expressing the coupling between two coupled antennas in terms of each antenna's spherical-wave source-scattering matrix representation. We go on to consider special results to substantiate our formulation, such as showing equivalence between the coupling equations for transmission in opposite directions when the antennas are reciprocal, showing uniform convergence of some series representations for antenna coupling and simultaneously obtaining a coordinate-system translation theorem for the dyadic Green's function, and showing that our two-antenna coupling equations reduce to expressions for the incident and emergent fields about a single antenna when the other antenna is an elementary dipole. Efficient probe-corrected spherical and hemispherical scanning algorithms are then developed for processing measured near-field data to obtain an antenna's far-field pattern. Finally, we describe a number of self-consistency tests and theoretical-data simulations that were developed to validate our spherical-scanning algorithm, and we describe an independent experimental verification.

[Contact: Richard L. Lewis, (303) 497-5196]

### Noise Metrology

Wait, D.F., **Radiometer Equation for Noise Comparison Radiometers**, IEEE Transactions on Instrumentation and Measurement, Vol. 44, No. 2, pp. 336-339 (April 1995).

A complete radiometer equation is derived and used to develop better corrections and uncertainty estimates. We believe it to be the first thorough analysis of radiometers with unisolated front ends. We show that a corrected unisolated radiometer can



have an accuracy similar to that of a well-isolated radiometer. The radiometer error is insignificant for radiometers with 40 dB isolation. However, for high-temperature applications (such as sources and standards above 3000 K), isolation is usually unnecessary.

[Contact: David F. Wait, (303) 497-3610]

#### Microwave and Millimeter-Wave Metrology

Clague, F.R., **A Calibration Service for Coaxial Reference Standards for Microwave Power**, NIST Technical Note 1374 (May 1995).

A calibration service at the National Institute of Standards and Technology for coaxial microwave power reference standards is described. The service provides measurements of the reference standard effective efficiency from 50 MHz to 18 GHz at a power level of 10 mW. In the Report of Calibration, the effective efficiency is reported in percent. The NIST microwave power standards consists of both a microcalorimeter and an associated reference standard. The reference standard is a bolometric-type power detector (a thermistor mount). The only thermistor mounts accepted for measurement are those constructed to NIST specifications which are compatible with the coaxial microcalorimeter. These thermistor mounts and the automated microcalorimeter are described. A detailed error analysis with an estimate of the calibration uncertainties and their sources is included. The calibration uncertainty, which is quoted as a function of frequency, ranges from about 0.2% at 50 MHz to 0.4% at 18 GHz.

[Contact: Fred R. Clague, (303) 497-5778]

DeGroot, D.C., Beall, J.A., Marks, R.B., and Rudman, D.A., **Microwave Properties of Voltage-Tunable  $\text{YBa}_2\text{Cu}_3\text{O}_{7-\delta}/\text{SrTiO}_3$  Coplanar Waveguide Transmission Lines**.

To explore the electrical characteristics of monolithic microwave circuits with integrated high-temperature superconductor and ferroelectric materials, we fabricated a series of coplanar waveguide transmission lines in laser-deposited  $\text{YBa}_2\text{Cu}_3\text{O}_{7-\delta}$  and  $\text{SrTiO}_3$  thin films. We characterized the voltage-tunable two-port microwave response of the transmission lines at cryogenic temperatures using a calibrated network analyzer system. Total phase

shifts and phase tuning in these devices increased for increasing ferroelectric film thickness with only moderate increases in transmission loss.

[Contact: Donald C. DeGroot, (303) 497-7212]

#### Electromagnetic Properties

Galt, D., Price, J.C., Beall, J.A., and Harvey, T.E., **Ferroelectric Thin Film Characterization Using Superconducting Microstrip Resonators**, IEEE Transactions on Applied Superconductivity, Vol. 5, No. 2, pp. 2575-2578 (June 1995).

We describe a novel technique for characterizing the dielectric response of ferroelectric thin films at microwave frequencies. The method involves a microstrip resonator which incorporates a ferroelectric capacitor at its center. To demonstrate this method, we have fabricated a superconducting microstrip resonator from a laser-ablated  $\text{YBa}_2\text{Cu}_3\text{O}_{7-\delta}$  film on a  $\text{LaAlO}_3$  (LAO) substrate with a  $\text{SrTiO}_3$  (STO) capacitor at its center. We report the observed dielectric behavior of the STO laser-ablated film as a function of bias at liquid He and  $\text{N}_2$  temperatures and at high and low frequencies. It is observed that the electrically tunable dielectric constant of the STO film is roughly independent of frequency up to 20 GHz (especially at high bias). The loss tangent of the STO/LAO capacitor decreases with increasing bias and is apparently independent of frequency between 6 and 20 GHz.

[Contact: James A. Beall, (303) 497-5989]

#### Laser Metrology

Leonhardt, R.W., and Scott, T.R., **Deep UV Excimer Laser Measurements at NIST**, Proceedings of SPIE (The International Society for Optical Engineering, P.O. Box 10, Bellingham, Washington 98227-0010), Integrated Circuit Metrology, Inspection, and Process Control IX, Vol. 2439, pp. 448-459 (1995).

The National Institute of Standards and Technology has designed and built two electrically calibrated laser calorimeters as primary standards for absolute energy measurements at the wavelength of 248 nm. Under the sponsorship of SEMATECH, NIST developed the calorimeters to improve measurement of dose-energy in excimer-laser-based microlithography. The calorimeter system

can be used to calibrate transfer standards which in turn can be used to calibrate detectors employed for energy measurements of semiconductor wafer exposure. The excimer calorimeter uses a glass filter which functions as a volume absorber that allows collection of nanosecond pulses of laser radiation without suffering damage. The measurement range of the calorimeters is 0.3 to 25 J, but can be extended to 1 mJ with beam splitters. Electrical calibration of the calorimeters shows a standard deviation in the calibration factor of less than 0.5% for entire energy range. The total uncertainty of typical power and energy meter calibrations is approximately 2%.

[Contact: Rodney W. Leonhardt, (303) 497-5162]

Zhang, Z.M., Livigni, D.J., Jones, R.D., and Scott, T.R., **Thermal Modeling and Analysis of Laser Calorimeters**, Proceedings of the 1995 ASME/AIAA National Heat Transfer Conference, Portland, Oregon, August 6-9, 1995, pp. 1-11.

We performed detailed thermal analysis and modeling of the C-series laser calorimeters at the National Institute of Standards and Technology for calibrating laser power or energy meters. A finite-element method was employed to simulate the space and time dependence of temperature at the calorimeter receiver. The inequivalence in the temperature response caused by different spatial distributions of the heating power was determined. The inequivalence between electrical power applied to front and rear portions of the receiver is  $\approx 1.7\%$ , and the inequivalence between the electrical and laser heating is estimated to be  $<0.05\%$ . The computational results are in good agreement with experiments at the 1% level. The effects of the deposited energy, power duration, and relaxation time on the calibration factor and cooling constant were investigated. This paper provides information for future design improvement on the laser calorimeters.

[Contact: David J. Livigni, (303) 497-5898]

#### Optical Fiber Metrology

Rappaport, A.G., Williams, P.A., Thomas, B.N., Clark, N.A., Ros, M.B., and Walba, D.M., **X-Ray Observation of Electroclinic Layer Constriction and Rearrangement in a Chiral Smectic-A Liquid Crystal**, Applied Physics Letters, Vol. 67,

No. 3, pp. 362-364, July 17, 1995.

An X-ray scattering study of electroclinic layer constriction verifies the interpretation of the electroclinic effect as field-induced molecular tilt. The tilt angles deduced from the layer spacing changes are in close agreement with those from optical measurements. Layer buckling, a consequence of the layer constriction, is also observed and may be the cause of the loss of optical contrast observed in electroclinic devices.

[Contact: Paul A. Williams, (303) 497-3805]

Williams, D.H., Young, M., and Tietz, L.A., **Fiber Coating Diameter: Toward a Glass Artifact Standard**, Proceedings of the 3rd Optical Fibre Measurement Conference, Liège, Belgium, September 25-26, 1995, p. III.2.

This paper proposes a glass fiber, 245  $\mu\text{m}$  in diameter, with an appropriate index of refraction as a standard for the calibration of outer primary coating diameter measurements. Fibers will be manufactured by either a melt process or a draw process. The index of refraction will be measured by the Becke line method and the diameter, with a contact micrometer.

[Contact: Matt Young, (303) 497-3223]

#### Optical Fiber/Waveguide Sensors

Patrick, H., and Gilbert, S.L., **Comparison of UV Photosensitivity and Fluorescence During Fiber Grating Formation**, Proceedings of the Photosensitivity and Quadratic Nonlinearity in Glass Waveguides: Fundamentals and Applications Topical Meeting, Portland, Oregon, September 9-11, 1995, pp. 148-151.

We have conducted a comparison of the UV photosensitivity of optical fiber with the blue fluorescence emitted during the exposure. In a survey of ten non-hydrogen-loaded germanium-doped fibers, we measured the UV photosensitivity and monitored the blue fluorescence during the growth of fiber gratings. Our goal was to determine whether the initial fluorescence, or the change in the fluorescence during exposure, is correlated with the index change. This provides insight into the underlying physical mechanism of UV-induced index change and also determines whether the blue

fluorescence can be used as an indicator of the photosensitivity of a fiber.

[Contact: Heather Patrick, (303) 497-6353]

Patrick, H., Gilbert, S.L., Lidgard, A., and Gallagher, M.D., **Annealing of Bragg Gratings in Hydrogen-Loaded Optical Fiber**, *Journal of Applied Physics*, Vol. 78, No. 5, pp. 2940-2945 (September 1995).

We have conducted a detailed study of the thermal stability of Bragg gratings written in hydrogen-loaded and unloaded germanium-doped optical fiber. Interference of either continuous-wave or pulsed ultraviolet light was used to induce the index modulation gratings. Some gratings were kept at room temperature and others were annealed at fixed temperatures for 10 to 20 h. For temperatures between room temperature and 350 °C, gratings in the hydrogen-loaded fiber showed significantly greater decay than those in the unloaded counterpart. The ultraviolet-induced index modulation in hydrogen-loaded fiber was reduced by 40% after 10 h at 176 °C, whereas it was reduced by only 5% in unloaded fiber under the same conditions. The annealing behavior of gratings written using the pulsed source was identical to that of gratings written with the continuous-wave source, and the thermal stability of gratings in hydrogen-loaded fiber did not depend on the magnitude of the index modulation. We also observed that the annealing of ultraviolet-induced OH absorption in the hydrogen-loaded fiber was not correlated with the grating decay. Our annealing results show that the species responsible for the index change in the hydrogen-loaded fiber are less stable than those in the unloaded fiber.

[Contact: Heather Patrick, (303) 497-6353]

Yang, S., Vayshenker, I., Li, X., Zander, M., and Scott, T.R., **Optical Detector Nonlinearity: Simulation**, NIST Technical Note 1376 (May 1995).

A unified mathematical treatment has been developed for five commonly used measurement methods of optical detector nonlinearity, and a computer simulation was conducted to compare these methods for different measurement conditions and data processing options. The triplet and differential methods are shown to give overall best

results, and third- and fourth-order polynomial representations of the measurement result will yield least total error for a common practical measurement system.

[Contact: Igor Vayshenker, (303) 497-3394]

### Integrated Optics

Graettinger, T.M., Morris, P.A., Roshko, A., Kingon, A.I., Auciello, O., Lichtenwalner, D.J., and Chow, A.F., **Growth of Epitaxial KNbO<sub>3</sub> Thin Films**, *Proceedings of the Materials Research Society Symposium*, Vol. 341, pp. 265-276 (1994).

KNbO<sub>3</sub> possesses high-nonlinear optical coefficients making it a promising material for frequency conversion of infrared light into the visible wavelength range using integrated optical devices. While epitaxial thin films of KNbO<sub>3</sub> have previously been grown using ion beam sputtering, defects (i.e., grain boundaries, domains, surface roughness) in these films resulted in high-optical losses and no measurable in-plane birefringence. Previous films were grown on MgO substrates, which have a >4% lattice mismatch with KNbO<sub>3</sub>. In the work reported here, we have grown films on MgO, MgAl<sub>2</sub>O<sub>4</sub>, and NdGaO<sub>3</sub> to investigate the role of lattice mismatch on the resulting film quality. Films have also been grown with and without oxygen ion assistance. The orientations, morphologies, and defects in the films were examined using X-ray diffraction and atomic force microscopy to determine their relationships to the growth conditions and substrate lattice mismatch.

[Contact: Alexana Roshko, (303) 497-5420]

Schaafsma, D.T., and Christensen, D.H., **Cross-Sectional Photoluminescence and Its Application to Buried-Layer Semiconductor Structures**, *Journal of Applied Physics*, Vol. 78, No. 2, pp. 694-699 (July 15, 1995).

[See Analysis and Characterization Techniques.]

Veasey, D.L., Malone, K.J., Aust, J.A., and Sanford, N.A., **Distributed Feedback Lasers in Rare-Earth-Doped Phosphate Glass**, *Proceedings of the 7th European Conference on Integrated Optics*, Delft, The Netherlands, April 3-6, 1995, pp. 579-581.

We have successfully demonstrated waveguide lasers operating at 1056.1, 1058.2, and 1062.6 nm in Nd-doped phosphate glass. The waveguides were fabricated by potassium ion exchange from a nitrate melt. Distributed feedback grating patterns were holographically written at 458 nm in photoresist spun on the sample surfaces. The gratings were developed, coated with chromium at a 60-degree evaporation angle, and were then transferred into the glass by argon ion sputtering. Typical laser threshold was 32 mW of absorbed pump power at 805 nm with a corresponding slope efficiency of 2%.

[Contact: David L. Veasey, (303) 497-5952]

Weisshaar, A., Gallawa, R.L., and Goyal, I.C., **Vector and Quasi-Vector Solutions for Optical Waveguide Modes Using Efficient Galerkin's Method with Hermite-Gauss Basis Functions**, Journal of Lightwave Technology, Vol. 13, No. 6, pp. 1795-1800 (August 1995).

An efficient vector formulation and a corresponding quasi-vector formulation for the analysis of optical waveguides are presented. The proposed method is applicable to a large class of optical waveguides with general refractive index profile in a finite region of arbitrary shape and surrounded by a homogeneous cladding. The vector formulation is based on Galerkin's procedure using Hermite-Gauss basis functions. It is shown that use of Hermite-Gauss basis functions leads to a significant increase in computational efficiency over trigonometric basis functions. The quasi-vector solution is obtained from the standard scalar formulation by including a polarization correction. The accuracy of the scalar, vector, and quasi-vector solutions is demonstrated by comparison with the exact solution for the fundamental mode in a circular fiber. Comparison of the modal solutions obtained with the various methods for optical waveguides with square, rectangular, circular, and elliptical core demonstrate the accuracy and advantage of the quasi-vector solution.

[Contact: Robert L. Gallawa, (303) 497-3761]

#### Other Signal Topics

Wieman, C., Flowers, G., and Gilbert S., **Inexpensive Laser Cooling and Trapping Experiment for Undergraduate Laboratories**, American

Journal of Physics, Vol. 63, No. 4, pp. 317-330 (April 1995).

We present detailed instructions for the construction and operation of an inexpensive apparatus for laser cooling and trapping of rubidium atoms. This apparatus allows one to use the light from low-power diode lasers to produce a magneto-optical trap in a low-pressure vapor cell. We present a design which has reduced the cost to less than \$3000 and does not require any machining or glassblowing skills in the construction. It has the additional virtues that the alignment of the trapping laser beams is very easy, and the rubidium pressure is conveniently and rapidly controlled. These features make the trap simple and reliable to operate, and the trapped atoms can be easily seen and studied. With a few milliwatts of laser power, we are able to trap  $4 \times 10^7$  atoms for 3.5 s in this apparatus. A step-by-step procedure is given for construction of the cell, setup of the optical system, and operation of the trap. A list of parts with prices and vendors is given in the Appendix.

[Contact: Sarah Gilbert, (303) 497-3120]

## ELECTRICAL SYSTEMS

### Power Systems Metrology

Martzloff, F.D., Mansoor, A., Phipps, K.O., and Grady, W.M., **Surging the Upside-Down House: Measurements and Modeling Results**, Proceedings of the Third International Conference on Power Quality End-Use Applications and Perspectives, Amsterdam, The Netherlands, October 24-27, 1994, Part 1, pp. A-1.05, 1-6. [Also, to be published in the Proceedings of the 1995 PQA Conference, New York, New York, May 8-11, 1995.]

Electronic equipment with two input ports, power and communications, can be exposed to damaging differences of voltage between the two ports during surge events. To demonstrate real-world scenarios, a replica of the wiring system in a typical residence was installed in the laboratory. This paper reports selected results from many measurements, and presents the corresponding numerical modeling, thereby leading to mutual validation of the two processes. Two exposure scenarios for producing differences of voltages between the power and data

ports of appliances are illustrated. Additional measurements and parametric variations are reported here to characterize the impedance of the various components of the wiring system and the source impedance of the resulting overvoltages appearing between the ports.

[Contact: François D. Martzloff, (301) 975-2409]

### Superconductors

Bray, S.L., Ekin, J.W., Waltman, D.J., and Superczynski, M.J., **Quench Energy and Fatigue Degradation Properties of Cu- and Al/Cu-Stabilized NbTi Epoxy-Impregnated Superconductor Coils**, IEEE Transactions on Applied Superconductivity, Vol. 5 - Part I, No. 2, pp. 222-225 (June 1995).

In comparative measurements of small-scale epoxy-impregnated Cu-stabilized and Al-Cu-stabilized NbTi test coils at 4 K and 5 T, the heat energy required to quench the Al-Cu-stabilized coil was 4 to 12 times greater than for the Cu-stabilized coil, depending on the relative operating current. Also, the coil's stabilizer resistivity ( $\rho$ ) was measured as a function of mechanical fatigue to test for strain-induced degradation. The  $\rho$  of the Cu-stabilized coil is relatively unaffected by fatigue, while that of the Al-stabilized coil increases with fatigue. However, in these coils, having a typical stabilizer:superconductor ratio of 4:1, the degradation of the Al-Cu-stabilized coil begins to saturate after several hundred fatigue cycles, and, after 2000 fatigue cycles to 0.2% strain, the  $\rho$  of the Al-Cu-stabilized coil is still 2.6 times lower than the  $\rho$  of the Cu-stabilized coil. Furthermore, after annealing the Al-Cu-stabilized coil at room temperature for 48 h, the  $\rho$  degradation was reduced by 76%. Thus, the use of Al-Cu-stabilizer may offer substantial improvements in magnet stability even where the magnet is subjected to fatigue degradation from repeatedly energizing the magnet.

[Contact: Steven L. Bray, (303) 497-5631]

Ekin, J.W., Russek, S.E., Clickner, C.C., and Sanders, S.C., **Oxygen Annealing of Ex-Situ YBCO/Ag Thin-Film Interfaces**, IEEE Transactions on Applied Superconductivity, Vol. 5 - Part III, No. 2, pp. 2400-2403 (June 1995).

The resistivity of YBCO/Ag interfaces has been

measured for different oxygen annealing temperatures for a series of ex-situ fabricated thin-film contacts having sizes ranging from  $16\ \mu\text{m} \times 16\ \mu\text{m}$  down to  $4\ \mu\text{m} \times 4\ \mu\text{m}$ . The interface resistivity began to decrease after annealing at 300 °C for 10 min. in one atmosphere oxygen. After annealing at 400 °C, the contact resistivity decreased by several orders of magnitude to the  $10^{-7}\ \Omega\text{-cm}^2$  range. The 500-nm thick Ag layer showed massive surface diffusion and agglomeration for annealing temperatures above 400 °C; this temperature, thus represents a practical limit for oxygen annealing the YBCO/Ag interface system for more than 10 min. Rapid cooling of the chip after annealing led to a severe loss of critical current density in the YBCO layer, which could be restored by reannealing and cooling at a slower rate of 50° C/min. The relative shape of the conductance-vs.-voltage characteristics of the YBCO/Ag interface were essentially unaltered by oxygen annealing; the overall parabolic shape, superconducting gap features, and magnetic-scattering zero bias anomaly remained constant, even though the contact conductance increased by several orders of magnitude. These data suggest that the main reduction in the interface resistivity arises from an enhancement of the effective contact area, not from a change in interface conduction mechanism.

[Contact: John W. Ekin, (303) 497-5448]

Goodrich, L.F., Wiejaczka, J.A., and Srivastava, A.N., **Anomalous Switching Phenomenon in Critical-Current Measurements When Using Conductive Mandrels**, IEEE Transactions on Applied Superconductivity, Vol. 5, No. 3, pp. 3442-3444 (September 1995).

NIST and other laboratories have observed an anomalous switching phenomenon that can occur in critical-current measurements of coiled Nb-Ti and Nb<sub>3</sub>Sn superconductors when mounted on an electrically-conductive measurement mandrel. During acquisition of the voltage-current (V-I) characteristic, large voltage discontinuities are observed. This switching phenomenon results in a multi-valued V-I curve, and apparently multiple "critical-current" values. An explanation of this phenomenon, some necessary conditions for the switching to occur, as well as methods of detecting the phenomenon, are given.

[Contact: Loren F. Goodrich, (303) 497-3143]

Goodrich, L.F., Wiejaczka, J.A., Srivastava, A.N., Stauffer, T.C., and Medina, L.T., **USA Interlaboratory Comparison of Superconductor Simulator Critical Current Measurements**, IEEE Transactions on Applied Superconductivity, Vol. 5, No. 2, pp. 548-551 (June 1995).

An interlaboratory comparison of critical current ( $I_c$ ) measurements was conducted on the superconductor simulator, which is an electronic circuit that emulates the extremely nonlinear voltage-current characteristic of a superconductor. These simulators are high-precision instruments, and are useful for establishing the integrity of part of a superconductor measurement system. This study includes measurements from participating U.S. laboratories, with NIST as the central, organizing laboratory. This effort was designed to determine the sources of uncertainty in  $I_c$  measurements due to uncertainties in the measurement apparatus, technique, or the analysis system. The participating laboratories measured the superconductor simulator with a variety of methods including dc and pulse. This comparison indicated the presence of systematic biases and higher variability at low voltages in the  $I_c$  determinations of the measurement systems. All critical current measurements at a criterion of 10  $\mu$ V on the  $I_c$  simulator were within 2% of the NIST value to nominal critical currents of 2 and 50 A. These results could significantly benefit superconductor measurement applications that require high-precision quality assurance.

[Contact: Loren F. Goodrich, (303) 497-3143]

Goodrich, L.F., Wiejaczka, J.A., Srivastava, A.N., Stauffer, T.C., and Medina, L.T., **First VAMAS USA Interlaboratory Comparison of High Temperature Superconductor Critical Current Measurements**, IEEE Transactions on Applied Superconductivity, Vol. 5, No. 2, pp. 552-555 (June 1995).

We conducted an interlaboratory comparison of critical current ( $I_c$ ) measurements on  $\text{Bi}_2\text{Sr}_2\text{Ca}_2\text{-Cu}_3\text{O}_{10}$  tapes (2223). This study includes measurements from six participating U.S. laboratories, with NIST as the central, organizing laboratory. A number of specimens were prepared with different degrees of instrumentation to isolate sources of variability. Most of the specimens were pre-measured by NIST to reduce uncertainties due to

sample variability. Different specimen routing patterns among the laboratories were implemented to isolate sources of variability due to the specimen's measurement history. This study is similar to other Versailles Project on Advanced Materials and Standards (VAMAS) intercomparisons being performed in Japan and Europe and is the first internationally cooperative interlaboratory comparison of HTS (High Temperature Superconductors)  $I_c$  measurements. These are the first steps towards developing standard measurement procedures for HTS.

[Contact: Loren F. Goodrich, (303) 497-3143]

McIntyre, P.C., Cima, M.J., and Roshko, A., **The Effects of Substrate Surface Steps on the Microstructure of Epitaxial  $\text{Ba}_2\text{YCu}_3\text{O}_{7-x}$  Thin Films on (001)  $\text{LaAlO}_3$** , Journal of Crystal Growth, Vol. 149, pp. 64-73 (1995).

The effects of steps in the (001) surface of  $\text{LaAlO}_3$  substrates on the microstructural evolution of heteroepitaxial  $\text{Ba}_2\text{YCu}_3\text{O}_{7-x}$  (BYC) thin films were characterized by high-resolution transmission electron microscopy and atomic force microscopy. Native substrate surface steps acted as nucleation sites for both the  $c$ -axis normal and  $c$ -axis in-plane ( $a$ -axis normal) orientations in BYC films prepared by post-deposition annealing of a precursor film. The density of  $c$ -axis in-plane BYC grains varied dramatically across the surface of the substrates. In several samples, the spatial pattern of  $c$ -axis in-plane regions present in the BYC films was similar to the twin structure present in the  $\text{LaAlO}_3$  substrates. Surface grooves present near twin boundaries in the substrates and lattice rotation of the  $\text{LaAlO}_3$  during its rhombohedral-cubic phase transition at  $\sim 450$  °C may produce the large surface steps that act as preferred sites for BYC nucleation.

[Contact: Alexana Roshko, (303) 497-5420]

Roshko, A., Russek, S.E., Trott, K.A., Sanders, S.C., Johansson, M.E., Martens, J.S., and Zhang, D., **Effects of Etching on the Morphology and Surface Resistance of  $\text{YBa}_2\text{Cu}_3\text{O}_{7-\delta}$  Films**, IEEE Transactions on Applied Superconductivity, Vol. 5 - Part II, No. 2, pp. 1733-1736 (June 1995).

The changes in surface morphology and surface resistance of sputtered and laser ablated

YBa<sub>2</sub>Cu<sub>3</sub>O<sub>7- $\delta$</sub>  films both before and after etching have been examined. Six different etchants were used: citric acid, nitric acid, Br-methanol, EDTA, disodium EDTA, and ion milling. The surface morphologies of the films were examined by reflection high-energy electron diffraction and atomic force microscopy, both before and after etching. The surface resistance ( $R_s$ ) was measured at 94 GHz using a confocal resonator. An amorphous layer was found on the film surfaces after exposure to air. A few of the etches restored some of the surface crystallinity, but most caused increases in the overall surface roughness. Several of the wet etches attacked dislocations. Ion milling caused the largest degradation of surface crystallinity and a corresponding increase in  $R_s$ . Some of the chemical etches increased  $R_s$  by less than 15%.  
[Contact: Alexana Roshko, (303) 497-5420]

Sanders, S.C., Russek, S.E., Clickner, C.C., and Ekin, J.W., **Evidence for Tunneling and Magnetic Scattering at In Situ YBCO/Noble-Metal Interfaces**, IEEE Transactions on Applied Superconductivity, Vol. 5 - Part III, No. 2, pp. 2404-2407 (June 1995).

We report low-temperature conductance data for in-situ YBa<sub>2</sub>Cu<sub>3</sub>O<sub>7- $\delta$</sub>  (YBCO)/Ag, YBCO/Au, and YBCO/Pt planar c-axis interfaces. Analysis of the conductance data for these interfaces, which have resistivities as low as  $1 \times 10^{-8} \Omega \text{ cm}^2$ , indicates that tunneling is the predominant transport mechanism. Zero-bias conductance peaks are present for all of the in-situ interfaces. These peaks are analyzed in the framework of the Appelbaum model and are attributed to the presence of isolated magnetic spins at the interface. The presence and similarity of the peaks for each noble-metal overlayer supports the hypothesis that the magnetic spins are inherent to the YBCO surface.

[Contact: Steven C. Sanders, (303) 497-5096]

Sanders, S.C., Sok, J., Finnemore, D.K., and Li, Q., **Thermally Activated Hopping of a Single Abrikosov Vortex**, Physical Review B, Vol. 47, No. 14, pp. 8996-9000 (1 April 1993-II).

Thermally activated hopping of a single Abrikosov vortex has been investigated for a thin Pb film that was decorated with an artificial pinning structure. To determine the location of the vortex, the Pb film

is fabricated to be one electrode of a cross-strip superconductor/normal-metal/insulator/superconductor Josephson junction. Distortions in the Fraunhofer pattern specify the vortex location. As the temperature is raised toward  $T_c$ , the vortex depins from the artificial pinning site and reproducibly moves through the same sequence of other pinning sites before it leaves the junction area of the Pb film. The first thermal depinning occurs when the order parameter of the bulk superconductor is about 20% of the  $T = 0$  value. The trajectory is not random.

[Contact: Steven C. Sanders, (303) 497-5096]

Voccio, J.P., Rodenbush, A.J., Joshi, C.H., Ekin, J.W., and Bray, S.L., **The Effect of Magnetic Field Orientation on the Critical Current of HTS Conductor and Coils**, IEEE Transactions on Applied Superconductivity, Vol. 5 - Part II, No. 2, pp. 1822-1825 (June 1995).

The critical current of short samples of high-critical-temperature superconductor multifilamentary conductor and ring-shaped coils has been measured at helium temperatures with varying magnetic field orientation with respect to the conductor. The samples and coil conductor consist of a multifilamentary composite of BSCCO-2223 filaments in a silver matrix. Short conductor samples were tested in a variable temperature system with up to 8 T background field using a sample rotational system. Ring-shaped coils made from the sample type of conductor were exposed to a large background field at liquid helium temperatures and critical current was measured with the ring located at various axial positions within the bore. As the ring moves closer to the end of the magnet, the measured critical current decreases, even though the magnitude of the field to which the ring is exposed decreases. This decrease in  $J_c$  is due to the strong anisotropy of the superconductor and is consistent with short sample measurements.

[Contact: John W. Ekin, (303) 497-5448]

#### Other Electrical Systems Topics

Christophorou, L.G., **Electron Attachment to Excited Molecules**, Proceedings of the International Symposium on Electron- and Photon-Molecule Collisions and Swarms, Berkeley, California, July 22-25, 1995, paper E-1.

The interactions of slow electrons with molecules, especially the processes of electron attachment, depend rather strongly on the internal energy content of the molecules themselves. As a rule, excited molecules interact with slow electrons with substantially larger cross sections than do ground-state molecules. Studies of electron attachment to vibrationally/rotationally excited, "hot," molecules and especially to electronically excited molecules are rather recent, in contrast to the extensive studies on electron attachment to ground-state molecules which cover many decades. Recent studies on electron attachment to thermally excited (or infrared-laser-excited vibrationally/rotationally excited) molecules showed that the effect of internal energy of a molecule on its electron attachment properties depends on the mode, dissociative or nondissociative, of electron attachment; and recent studies of electron attachment to electronically excited molecules, especially photoenhanced dissociative electron attachment to short- and long-lived excited electronic states of molecules produced directly or indirectly by laser irradiation, are discussed.

[Contact: Loucas G. Christophorou, (301) 975-2432]

## ELECTROMAGNETIC INTERFERENCE

### Conducted EMI

#### Recently Published

Martzloff, F.D., Mansoor, A., Phipps, K.O., and Grady, W.M., **Surging the Upside-Down House: Measurements and Modeling Results**, Proceedings of the Third International Conference on Power Quality End-Use Applications and Perspectives, Amsterdam, The Netherlands, October 24-27, 1994, Part 1, pp. A-1.05, 1-6. [Also, to be published in the Proceedings of the 1995 PQA Conference, New York, New York, May 8-11, 1995.]

[See Power Systems Metrology.]

## ADDITIONAL INFORMATION

### Announcements

#### **Characterization Workshop Proceedings Published**

The Proceedings of the International Workshop on Semiconductor Characterization: Present Status and Future Needs is now available through AIP Press. The book *Semiconductor Characterization* covers the unique characterization requirements of both silicon IC development and manufacturing and compound semiconductor materials, devices, and the National Technology Roadmap for Semiconductors. Additional sections discuss technology trends and future requirements for compound semiconductor applications. Recent developments in characterization, including in-situ, in-FAB, and off-line analysis methods are also highlighted. The book provides useful insights on the capabilities of different characterization techniques, gives perspectives on industrial metrology requirements, and explores critical needs and issues in semiconductor metrology research. This book will serve as a base-line reference in this rapidly growing field for the next decade.

In the foreword, **Craig Barrett**, Chief Operating Officer at Intel, and **Arati Prabhakar**, Director of NIST, stated that "characterization and modeling of semiconductors are increasingly becoming a crucial part of semiconductor manufacturing. This book provides a concise and effective portrayal of industry characterization needs and the problems that must be addressed by industry, government, and academia to continue the dramatic progress in semiconductor technology."

The work is based on papers given at the International Workshop, held the week of January 30, 1995 at NIST in Gaithersburg, Maryland. Sponsors were: The Advanced Research Projects Agency, SEMATECH, the National Institute of Standards and Technology, The Army Research Office, the U.S. Department of Energy, the National Science Foundation, Semiconductor Equipment and Materials International (SEMI), the Manufacturing Science and Technology Division of the American Vacuum Society, and the Working Group on Electronic Materials of the Committee on Civilian



### Dr. David G. Seiler Appointed Chief of NIST's Semiconductor Electronics Division

On September 1, 1995, David G. Seiler assumed the responsibilities of Chief of the Semiconductor Electronics Division, Electronics and Electrical Engineering Laboratory, at the National Institute of Standards and Technology. Dr. Seiler has been with the Division as leader of the Materials Technology Group since 1988, with an assignment as a NIST Program Office analyst for the past year. Prior to coming to NIST, Seiler was a Regents Professor of Physics at the University of North Texas, had served as a solid state physics program officer in the Division of Materials Research at the National Science Foundation (1985-86), and spent a year's sabbatical at the M.I.T. Francis Bitter National Magnet Laboratory (1980-81). Seiler has made significant contributions to the characterization of various semiconductors and has published over 100 papers on their electrical, optical, and nonlinear optical properties. He also has organized a number of international conferences and workshops on semiconductors and has been the editor of several semiconductor books.

The Semiconductor Electronics Division provides measurement-related infrastructure needed by the semiconductor industry in the areas of semiconductor materials, processing, and integrated circuits. Seiler wants the division to continue to make a significant impact on the semiconductor industry with respect to silicon, through achieving goals outlined in the 1994 Semiconductor Industry Association National Technology Roadmap for Semiconductors. With respect to compound semiconductors, he wants to help industry develop an assessment of the measurement infrastructure required for advances in compound semiconductors, and then help to respond to this assessment.

Industrial Technologies.

[Contact: Ann G. Bradford, (303) 497-3678]

For additional information, or to order the Proceedings, call the American Institute of Physics toll free at 1-800-809-2247.

Lyons, R.M., **A Bibliography of the NIST Electromagnetic Fields Division Publications**, NISTIR 5039 (August 1995).

#### Lists of Publications

Bradford, A.G., **Metrology for Electromagnetic Technology: A Bibliography of NIST Publications**, NISTIR 5040 (September 1995).

This bibliography lists the publications by the staff of the National Institute of Standards and Technology's Electromagnetic Fields Division for the period January 1970 through July 1995. It supersedes NISTIR 5028 which listed the publications of the Electromagnetic Fields Division from January 1970 through July 1994. Selected earlier publications from the Division's predecessor organizations are included.

[Contact: Ruth Marie Lyons, (303) 497-3132]

This bibliography lists the publications of the personnel of the Electromagnetic Technology Division of NIST during the period from January 1970 through publication of this report. A few earlier references that are directly related to the present work of the Division are also included. This edition of the bibliography is the first since the Electromagnetic Technology Division split into two Divisions, and it includes publications from the areas of cryoelectronic metrology and superconductor and magnetic measurements. The optical electronic metrology section found in earlier editions is now being produced separately by the new Optoelectronics Division of NIST. That companion bibliography to this publication is NISTIR 4041.

Schmeit, R.A., **Electrical and Electronic Metrology: A Bibliography of NIST Electricity Division's Publications**, NIST List of Publications 94 (July 1995).

This bibliography covers publications of the Electricity Division (and predecessor organizational units), Electronics and Electrical Engineering Laboratory, National Institute of Standards and Technology, for the period of January 1968 through

December 1994. A brief description of the Division's technical program is given in the introduction.

[Contact: Ruth A. Schmeit, (301) 975-2401]

Smith, A.J., and Derr, L.S., **A Bibliography of Publications of the NIST Optoelectronics Division**, NISTIR 5041 (September 1995).

This bibliography lists publications of the staff of the Optoelectronics Division and its predecessor organizational units from 1970 through the date of this report.

[Contact: Annie J. Smith, (303) 497-5342]

Walters, E.J., **NIST List of Publications 103, National Semiconductor Metrology Program and the Semiconductor Electronics Division, 1990-1995** (March 1996).

This List of Publications includes all papers relevant to semiconductor technology published by NIST staff, including work of the National Semiconductor Metrology Program and the Semiconductor Electronics Division, and other parts of NIST having independent interests in semiconductor metrology. Bibliographic information is provided for publications from 1990 through 1995. Indices by topic area and by author are provided. Earlier reports of work performed by the Semiconductor Electronics Division (and its predecessor divisions) during the period from 1962 through December 1989 are provided in NIST List of Publications 72.

[Contact: E. Jane Walters, (301) 975-2050]

### 1996 Calendar of Events

#### **May 6-7, 1996 (Baveno, Italy)**

#### **IEEE Workshop on VLSI and Microsystem Packaging Techniques and Manufacturing.**

The Workshop is co-sponsored by NIST and IEEE, in cooperation with the European Communities, ESPRII DGIII-Industry, NETPACK (the Network in Microelectronic System Integration Packaging), and the JESSI Organization. Topics to be addressed are: the design and implementation of first-level electronic packaging and the technologies, materials, and equipment for the manufacture of multichip and single-chip packages for VLSI and the

new emerging domain of microsensors and microsystems.

[Contact: George G. Harman, (301) 975-2097]

#### **July 16-18, 1996 (San Francisco, California)**

**SEMICON/West '96, Moscone Center.** The NIST National Semiconductor Metrology Program will continue its government-industry liaison support role by exhibiting at SEMICON/West in 1996. For over 40 years, NIST and its predecessor, the National Bureau of Standards, have provided expertise on semiconductor-related issues to industry, government agencies, and academia. Since SEMICON/West's inception 26 years ago, NIST personnel have provided the same expertise to the show's attendees. NIST's booth is located in Hall 4, Booth 6547. Please stop by and see us!

[Contact: Alice Settle-Raskin, (301) 975-4400]

#### **October 1-3, 1996 (Boulder, Colorado)**

#### **Symposium on Optical Fiber Measurements.**

This Symposium, held at NIST in Boulder, provides a forum for reporting the results of recent measurement research in the area of lightwave communications, including optical fibers. Aspects of optical fiber metrology will be discussed, including attenuation, dispersion, geometry, reflectometry, and connectors; integrated optic devices; laser diode sources and detectors; system measurements; and standards.

[Contact: Douglas L. Franzen, (303) 497-3346]

### EEEL Sponsors

National Institute of Standards and Technology  
Executive Office of the President

U.S. Air Force

Hanscom Air Force Base; McCellan Air Force Base; Newark Air Force Base; Patrick Air Force Base; Combined Army/Navy/Air Force (CCG); CCG-Strategic Defense Command; CCG-Systems Command; Wright Patterson

U.S. Army

Fort Belvoir; Redstone Arsenal; Combined Army/Navy/Air Force (CCG)

Department of Defense

Advanced Research Projects Agency; Defense Nuclear Agency; National Security Agency

Department of Energy

Building Energy R&D; Energy Systems Research; Fusion Energy; Basic Energy Sciences  
Department of Justice  
Law Enforcement Assistance Administration  
U.S. Navy  
CCG, Seal Beach; Office of Naval Research;  
Naval Research Laboratory; Commanding  
Officer-San Diego; Naval Surface Warfare  
Center; Naval Air Systems Command  
National Science Foundation

National Aeronautics and Space Administration  
NASA Headquarters  
Department of Transportation  
National Highway Traffic Safety Administration  
MMIC Consortium  
Nuclear Regulatory Commission  
Department of Health and Human Services  
National Institutes of Health  
Various Federal Government Agencies

## NIST SILICON RESISTIVITY SRMs

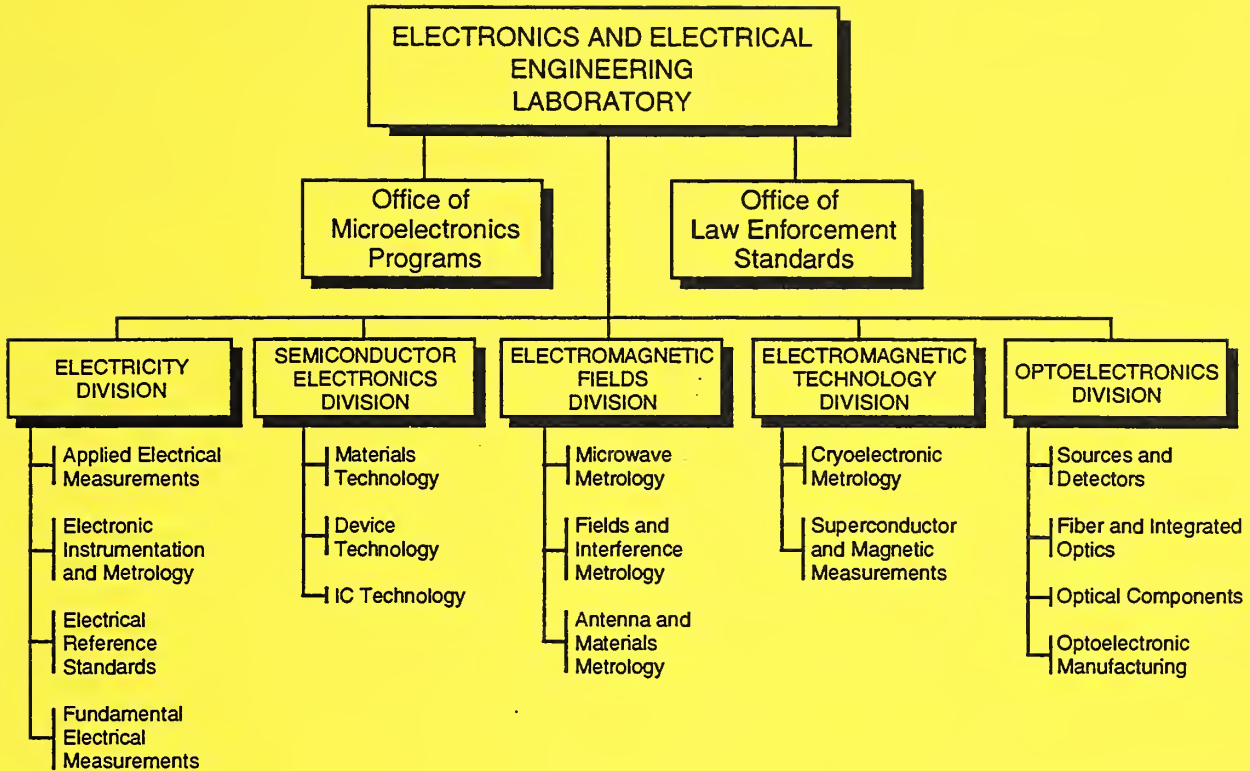
The Semiconductor Electronics Division of NIST provides Standard Reference Materials (SRMs) for bulk silicon resistivity through the NIST Standard Reference Materials Program. The existing SRMs (on 50 mm wafers) shown in the table below will be augmented with an improved set (on 100 mm wafers) during CY 96-97. NIST efforts to produce the new SRMs have recently received increased emphasis. The earlier set will continue to be available until the supply is exhausted.

The new SRMs have similar values of nominal resistivity as the earlier set, but offer improved uniformity and substantially reduced uncertainty of certified values due both to material and procedural improvements. While it is expected that these wafers will offer considerable utility in calibrating contactless gauges, certification has been performed solely with four-point probe methods. Technical insights presented by the rigorous certification process will be presented in a NIST Special Publication. Individual data for each wafer will be supplied along with the SRM Certificate.

It is expected that the higher resistivity SRMs (2547, 2546) will be available first during CY 96 and be followed closely by SRM 2545. The low resistivity material (SRMs 2542, 2541) is expected to be available by year end. A limited number of SRM 2543 may also be available by year end, with the remainder in early CY 97. Technical issues associated with SRM 2544 will preclude its availability until CY 97.

<b><i>NIST SILICON BULK RESISTIVITY STANDARD REFERENCE MATERIALS</i></b>				
DATE UPDATED: 23 JANUARY 1996				
NOMINAL RESISTIVITY (ohm · cm)	<u>OLD SRMs</u>	AVAILABILITY	<u>NEW SRMs</u> (ohm · cm)	ANTICIPATED AVAILABILITY
0.01	1523 (one of set of two wafers)	limited supply	2541	CY 96
0.1	1521 (one of set of two wafers)	limited supply	2542	CY 96
1	1523 (one of set of two wafers)	limited supply	2543	CY 96-97
10	1521 (one of set of two wafers)	limited supply	2544	CY 97
25	1522	set of three wafers no longer available	2545	CY 96
75	1522		2546 (100)	CY 96
180	1522		2547 (200)	CY 96

The above table will be updated in future issues to reflect changes in availability. Every effort will be made to provide accurate statements of availability; NIST sells SRMs on an as-available basis. For technical information, contact James R. Ehrstein, (301) 975-2060; for ordering information, call the Standard Reference Materials Program Domestic Sales Office: (301) 975-6776.



### KEY CONTACTS

Laboratory Headquarters (810)

Director, Judson C. French (301) 975-2220  
 Deputy Director, Robert E. Hebner (301) 975-2220  
 Associate Director, Alan H. Cookson (301) 975-2220

Office of Microelectronics Programs

Director, Robert I. Scace (301) 975-4400

Office of Law Enforcement Standards

Director, Kathleen M. Higgins (301) 975-2757

Electricity Division (811)

Acting Chief, William E. Anderson (301) 975-2400

Semiconductor Electronics Division (812)

Chief, David G. Seiler (301) 975-2054

Electromagnetic Fields Division (813)

Chief, Allen C. Newell (303) 497-3131

Electromagnetic Technology Division (814)

Acting Chief, Richard E. Harris (303) 497-3776

Optoelectronics Division (815)

Chief, Gordon W. Day (303) 497-5204

### INFORMATION:

For additional information on the Electronics and Electrical Engineering Laboratory, write or call:

Electronics and Electrical Engineering Laboratory  
 National Institute of Standards and Technology  
 Metrology Building, Room B-358  
 Gaithersburg, MD 20899  
 Telephone: (301) 975-2220

